

Transmitters and receivers in SiGe BiCMOS technology for sensitive gas spectroscopy at 222 - 270 GHz

Cite as: AIP Advances 9, 015213 (2019); <https://doi.org/10.1063/1.5066261>

Submitted: 13 October 2018 . Accepted: 02 January 2019 . Published Online: 16 January 2019

K. Schmalz , N. Rothbart, M. H. Eissa, J. Borngräber, D. Kissinger, and H.-W. Hübers 



View Online



Export Citation



CrossMark



Don't let your writing keep you from getting published!

AIP | Author Services

Learn more today!



Transmitters and receivers in SiGe BiCMOS technology for sensitive gas spectroscopy at 222 - 270 GHz

Cite as: AIP Advances 9, 015213 (2019); doi: 10.1063/1.5066261

Submitted: 13 October 2018 • Accepted: 2 January 2019 •

Published Online: 16 January 2019



K. Schmalz,^{1,a)}  N. Rothbart,^{2,3} M. H. Eissa,¹ J. Borngräber,¹ D. Kissinger,^{1,4} and H.-W. Hübers^{2,3} 

AFFILIATIONS

¹IHP – Leibniz-Institut für Innovative Mikroelektronik, Im Technologiepark 25, 15236 Frankfurt (Oder), Germany

²Deutsches Zentrum für Luft- und Raumfahrt (DLR), Institute of Optical Sensor Systems, Rutherfordstr. 2, 12489 Berlin, Germany

³Humboldt-Universität zu Berlin, Institute of Physics, Newtonstraße 15, 12489 Berlin, Germany

⁴Technische Universität Berlin, 10623 Berlin, Germany

^{a)}Electronic mail: schmalz@ihp-microelectronics.com.

ABSTRACT

This paper presents transmitter and receiver components for a gas spectroscopy system. The components are fabricated in IHP's 0.13 μm SiGe BiCMOS technology. Two fractional-N phase-locked loops are used to generate dedicated frequency ramps for the transmitter and receiver and frequency shift keying for the transmitter. The signal-to-noise ratio (SNR) for the absorption line of gaseous methanol (CH_3OH) at 247.6 GHz is used as measure for the performance of the system. The implemented mixer-first receiver allows a high performance of the system due to its linearity up to an input power of -10 dBm. Using a transmitter-array with an output power of 7 dBm an SNR of 4660 (integration time of 2 ms for each data point) was obtained for the 247.6 GHz absorption line of CH_3OH at 5 Pa. We have extended our single frequency-band system for 228 – 252 GHz to a 2-band system to cover the range 222 – 270 GHz by combining corresponding two transmitters and receivers with the frequency bands 222 – 256 GHz and 250 – 270 GHz on single transmitter- and receiver-chips. This 2-band operation allows a parallel spectra acquisition and therefore a high flexibility of data acquisition for the two frequency-bands. The 50 GHz bandwidth allows for highly specific and selective gas sensing.

© 2019 Author(s). All article content, except where otherwise noted, is licensed under a Creative Commons Attribution (CC BY) license (<http://creativecommons.org/licenses/by/4.0/>). <https://doi.org/10.1063/1.5066261>

I. INTRODUCTION

Spectroscopy at mm-wave (mmW)/terahertz (THz) frequencies is a very powerful tool for high resolution gas spectroscopy because many molecules have rotational transitions in the mmW/THz range.^{1,2,4-8} With mmW/THz gas spectroscopy it is possible to detect a large number of molecules. Therefore this technique can provide a profile of volatile organic compounds (VOCs) and toxic industrial chemicals (TICs) in air.^{2,3,8}

Recently, significant progress has been made in sources based on frequency synthesis techniques starting with a fundamental oscillator in the region around 10 GHz and subsequent frequency multiplication. This has led to the

development of mmW/THz spectrometers for molecular absorption spectroscopy.^{1,2}

Typically, these spectrometers use a continuous wave solid state harmonic multiplier based on GaAs Schottky diodes operating in combination with a matching heterodyne detection system. The source and the detector are driven by a microwave synthesizer. The disadvantage of these spectrometers is the high cost of its components. The implementation of integrated mmW/THz components in SiGe BiCMOS or CMOS technology offers a path towards a compact and low-cost system for gas spectroscopy.

Previously, we demonstrated transmitters (TXs) and receivers (RXs) fabricated in IHP's 0.13 μm SiGe BiCMOS

technology with integrated antennas for gas spectroscopy at 238 - 252 GHz,⁹⁻¹² and 494 - 500 GHz,¹³ using integer-N phase-locked loops (PLLs). The designs of the TX- and RX-chips are described in detail.⁹⁻¹¹ A more compact TX/RX system with fractional-N PLLs allowed frequency ramps in the range 238 - 252 GHz for the TX and RX, and for the TX a superimposed frequency modulation using frequency shift keying (FSK).¹⁴ This configuration allows also for switching between preselected frequency regions according to the spectral signature, thus reducing the data acquisition time considerably by a factor up to 10.¹¹ Recently, a 220-320 GHz spectrometer has been described, which consists of a pair of 65-nm CMOS chips, which utilizes two frequency-comb signals with ten equally spaced frequency tones to scan the spectrum.^{15,16}

In a recent development, we extended our single-band TX/RX system to a 2-band system to cover the range 225 - 273 GHz.¹⁷ It is built on one board by combining corresponding pairs of TX- and RX-chips of two frequency bands. This 2-band operation allows parallel spectra acquisition for these two bands. We have demonstrated a two-channel gas spectroscopy setup based on two TX-chips on the board and a single RX-chip. The channel discrimination was realized by different modulation frequencies,¹⁸ or by the intermediate frequencies (IFs) using corresponding band pass filters.¹⁹ Since two separate TX-chips are used, the optical coupling to the RX-chip was not optimal due to the relatively large distance between the antennas of the two single TX-chips. The use of two transmitters combined on a single TX-chip would improve significantly the coupling to the receiver and therefore the SNR. Further, with two appropriate TXs on a single TX-chip and two receivers on a single RX-chip an effective 2-band system can be realized.

This paper presents a 2-band TX-chip and a 2-band RX-chip, which are implemented by combining two TXs and two RXs on corresponding single chips, to realize an effective bandwidth of 220 - 270 GHz for our spectroscopy system. We further show, that a mixer-first receiver has improved the performance of our spectroscopy system due to its higher linearity compared to our previous RX as demonstrated by a signal-noise ratio of 4660 for the 247.6 GHz absorption line of CH₃OH at 5 Pa. Using our previous TX/RX system we obtained

only a maximum SNR of 1515 (integration time of 2 ms for each data point) for the 241.7 GHz absorption line of CH₃OH at 1.4 Pa, which has nearly the same absorption strength.¹⁷ (The absorption coefficients of the 241.7 GHz and 247.6 GHz absorption lines of CH₃OH are nearly equal).

The paper is organized as follows: The 2-band TX and RX circuits for our mmW/THz system are presented in Section II, followed by a presentation of system aspects in Section III. Section IV is dedicated to our recent results on gas spectroscopy, and Section V provides a discussion of these results. The paper ends with some conclusions concerning further improvement of our TX/RX system and its realization.

II. TRANSMITTER AND RECEIVER IN SiGe CMOS

The TX and RX circuits for our gas spectroscopy are fabricated in IHP's 0.13 μ m SiGe BiCMOS technology with f_T/f_{max} of 300/500 GHz.²⁰ The TX and RX include a local oscillator (LO), whose frequency is tuned by an external fractional-N PLL device.

A. Local oscillators for the frequency range from 222 to 270 GHz

The LO consists of a push-push voltage controlled oscillator (VCO) with a frequency divider, and a differential two-stage power amplifier, which is connected to a frequency doubler. The push-push VCO is a harmonic oscillator, which consists of two sub-oscillators in common-collector topology. In the line to the supply-voltage a transformer is placed, which transfers the signal to a differential cascode buffer with transformer-coupled output.²⁴ Accordingly, we developed two VCOs for the tuning ranges: a) 111 - 128 GHz, and b) 125 - 135 GHz. The output power of the VCO is about 1 dBm at 120 GHz for supply voltage of 3.3 V and DC current of 32 mA. The phase noise of the VCO at 120 GHz was estimated to be better than -91 dBc/Hz at 1 MHz offset using the measured phase noise at the 1/64 divider output. The phase noise of the VCO at 120 GHz gives -85 dBc/Hz at the doubled frequency for the TX.¹¹ Fig. 1 shows the schematic of the LO without the frequency divider. The 1/64 frequency divider is

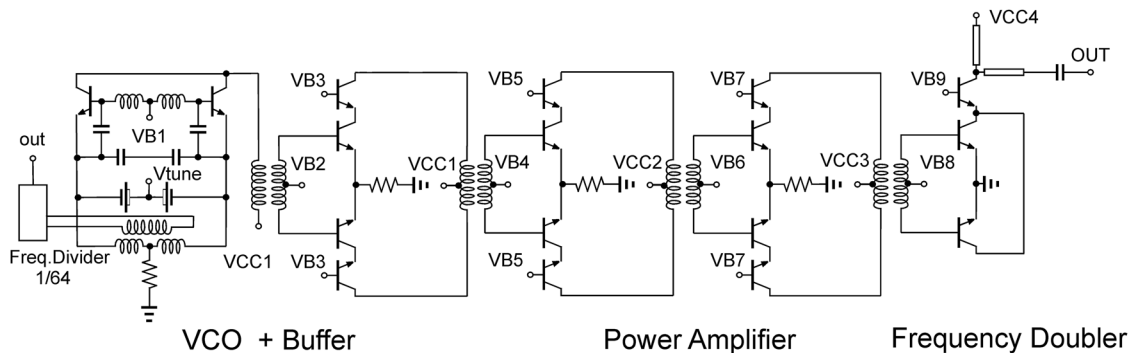


FIG. 1. Schematic of the LO with the VCO, and the two-stage power amplifier coupled to the frequency doubler.

coupled inductively to the VCO core at the fundamental frequency, and the LO-frequency is tuned by an external PLL device. The 1/64 frequency divider consists of a cascade of six static divider stages (divide-by-2) in CML (current-mode logic) using also SiGe HBTs for the divide-by-2 stages at low frequency. The currents and the sizes of SiGe HBTs in the divider stages are scaled down for the following stages with lower frequency to reduce power dissipation. The frequency divider draws 40 mA at supply voltage of 3.3 V. We obtained reliable frequency locking of the VCO for a divider frequency range of 55 – 67.5 GHz.

In order to cover a frequency range of 220 – 270 GHz, we have extended our previous single-band TX/RX system for 238 – 252 GHz to a 2-band system. The LOs of the TX and RX have been modified to extend the frequency range. In our 2-band system, corresponding pairs of TX and RX of the two frequency bands are combined. Fig. 2 presents the output frequencies of two LOs for the frequency range 220 – 270 GHz as a function of their tuning voltage. The LOs for the range 222 – 270 GHz are based on the same topology, but the parameters of their VCOs were optimized to realize the following two frequency bands a) 222–256 GHz, and b) 250–270 GHz.

Fig. 3 shows the block-diagram of our 2-band system with two TXs on one chip, two RXs on one chip, and four external PLL-circuits for frequency tuning of the four LOs.

B. Transmitters for the range 222 – 270 GHz

The single TX consists of a LO, which is connected to an on-chip antenna. Our previous spectroscopic system for the frequency range 238 – 252 GHz includes a single TX with 0 dBm output power and 7 dBm effective isotropically radiated power (EIRP) at 245 GHz.¹¹ We have developed a TX-array for the same frequency range, which delivers +7 dBm output power and 18 dBm EIRP at 245 GHz.¹⁰ This array includes four TXs for spatial power combining. Each TX consists of a

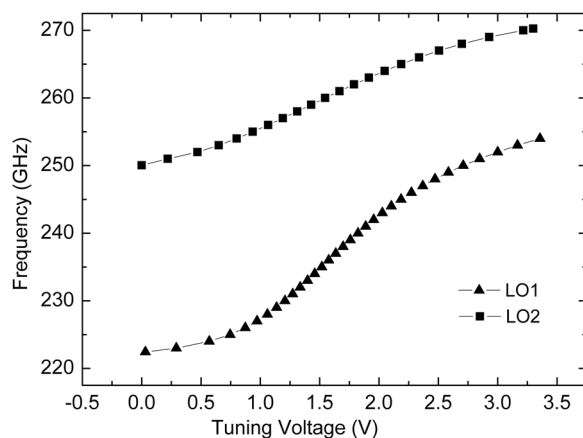


FIG. 2. Frequency of the LO is depicted as function of the tuning voltage of their VCOs. Two versions of the LO are realized with the following frequency ranges: a) LO1: 222–256 GHz, and b) LO2: 250–270 GHz.

two-stage power amplifier, followed by a frequency doubler, which is connected to an on-chip antenna. The inputs of these TXs are connected to a Wilkinson power divider network, which is fed by a LO.

In this work, we have built two TXs in correspondence to the two LOs for the frequency bands a) 222–256 GHz, and b) 250–270 GHz. The two TXs with the LO1 and LO2, respectively, are combined in a single chip as a 2-band TX to cover the frequency range 222 – 270 GHz, see Fig. 4. Here, the two on-chip antennas are connected to the outputs of LO1 and LO2, respectively. We have used the same LOs with identical layouts also for a 2-band receiver, see Fig. 5.

We have used LBE (Localized Backside Etching) available at IHP as option of technology way to improve the efficiency of the on-chip antenna by removing the lossy silicon under the radiator. The top thick layer TM2 is used to realize two

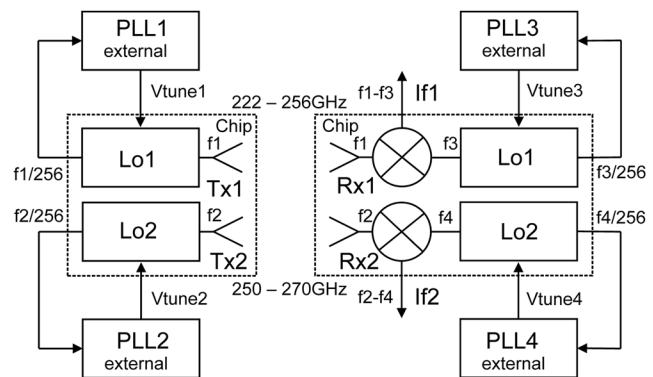


FIG. 3. Block diagram of the 2-band TX/RX system with the two frequency ranges: a) 222–256 GHz, and b) 250–270 GHz.

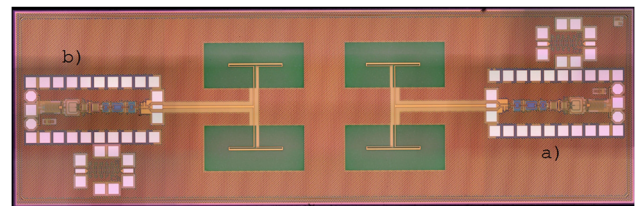


FIG. 4. Photograph of the 2-band transmitter chip for 220 – 270 GHz with two TXs for the frequency bands a) 222–256 GHz, and b) 250–270 GHz. (The small circuits at the right and left side are not related to the TX).

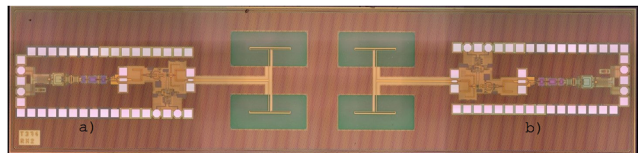


FIG. 5. Photograph of the 2-band receiver with two receivers with the LOs for the frequency bands a) 222–256 GHz, and b) 250–270 GHz.

half-wavelength folded dipoles and the feeding transmission lines. The two LBE antennas require a relatively large ground planes on top of the silicon substrate, which causes about 50% of chip-area to be empty, see Figs. 4 and 5.

C. Receivers for the range 222 – 270 GHz

A mixer-first receiver is used, with dc offset cancellation loop architecture to compensate for the mixer dc offsets and biasing purposes as described in Ref. 21. A transimpedance amplifier is utilized as a load for the mixer, which is optimized with a dc offset cancellation loop to maximize the bandwidth. This reported RX achieves a 3-dB bandwidth of 55 GHz, with a conversion gain of 13 dB, and a measured average single-sideband noise figure is 18 dB.²¹

We combined the core of this RX with our three LOs to build three RXs for the corresponding frequency ranges of the LOs. The receivers with the LO1 and LO3, respectively, are combined on a single chip as a 2-band RX for the two bands 222–256 GHz and 250–270 GHz to cover the frequency range 222 – 270 GHz, see Fig. 5.

Fig. 6 shows the effective output power of the LOs as function of their frequency, which was obtained by on-wafer measurements of the 2-band RX using probes at the outputs of the LO1 and LO3, respectively, whereby the supply voltage of the RX core was switched off. The frequency of the LO was set by tuning the voltage of its VCO. The small ripple in the output power should be related to a calibration problem of the probes.

The same mixer of or RX was presented previously for a wideband direct-conversion RX, where a LO chain that multiplies by 8 an external 30-GHz input signal drives the mixer, see Ref. 21. To characterize the mixer of our RX on wafer we applied first an external 240 GHz LO signal using a frequency extender with probe on the corresponding input pad. Then we switched on the internal LO, which frequency is tuned by

external voltage of its VCO, and is sufficient stable during the measurement. Here, a phase locking of VCO is not possible on wafer, but realized for spectroscopic measurements using a PCB module with external PLL device.

Two cascaded, resistively loaded common emitter amplifiers are utilized after the TIA to further increase the voltage gain and drive the external 100-ohm-load.²¹ The receiver was measured on wafer. A conversion gain of 13 dB was measured with a 3-dB BW of 55 GHz. The noise figure was measured using the gain method, achieving an average SSB NF of 18 dB. Therefore, the conversion gain and the SSB NF do not change significantly from IF frequency of 1 GHz, as used for the characterization, to the IF frequency of 2.15 GHz in our spectroscopic measurements (see below). The conversion gain and the SSB noise figure do not include the antenna efficiency. For the used antenna, we obtained by simulation that the efficiency is better than 75% with a gain of more than 7 dBi at the frequency range 235 – 255 GHz.¹⁷

Fig. 7 shows the effective conversion gain of these RXs at an IF-frequency of 1 GHz as function of their RF frequencies, which was obtained by using probes at the inputs of the RX cores. The LO-frequency of the RX is used as parameter. The LO-frequency was set by tuning the voltage of its VCO. Here, the on-chip antenna is connected in parallel to the RX input, and therefore the effective conversion gain is shaped by the characteristics of the antenna.

Fig. 8 shows the IF-output power of the RX at an IF-frequency of 1 GHz as function of the RF-input power at 240 GHz. The on-wafer measurement was performed using an external LO with an output power of -4 dBm at 241 GHz. The internal LO of the RX was switched off during this measurement. Considering the loss of the probe, the LO power at the RX core was only about -6.5 dBm compared to the output power of the internal LO, see Fig. 6. This explains the lower conversion gain of about 6 dB compared to the value of 13 dB

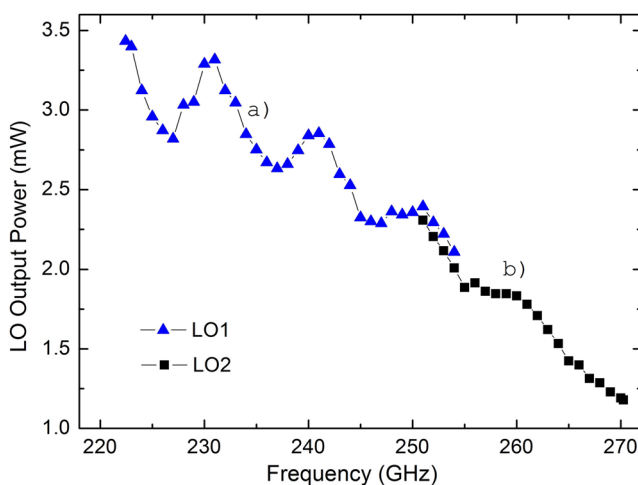


FIG. 6. Output power of the two LOs for the frequency bands: a) 222-256 GHz, and b) 250-270 GHz.

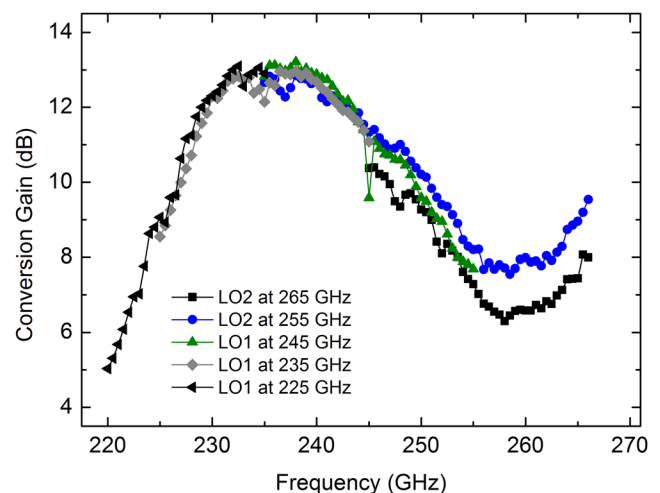


FIG. 7. Effective conversion gain of the receivers.

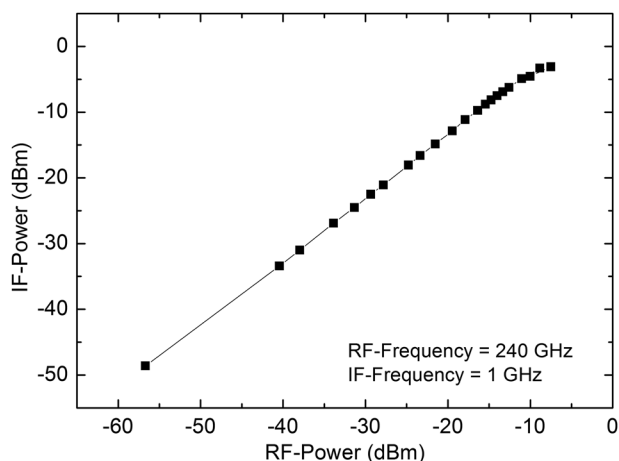


FIG. 8. The IF-power of the receiver is shown as function of the RF-power for RF-frequency of 240 GHz and IF-frequency of 1 GHz.

in Fig. 7. The RX exhibits a high linearity with an input 1-dB compression point of about -10 dBm.

III. SYSTEM FOR GAS SPECTROSCOPY

A. Modules for the transmitter and receiver with PLL

The TX/RX chips were bonded on a plug-in board, which was mounted on a baseband board. The boards were then screwed in front of the HDPE windows of the gas absorption cell, which serve as lenses. The baseband board contains multiple linear voltage regulators to supply all of the chips' bias voltages from a single 5 V DC supply, an amplifier to amplify the divider output of the LOs of TX and RX to the level required by PLL, and a loop filter to determine the loop stability of the PLL circuitry. The PLL device (Analog Device ADF4159) was not yet integrated on our first version of the baseband board, and instead a PLL evaluation boards (Analog Devices EV-ADF4159EB3Z) were connected to the baseband board by SMA cables.¹⁷

The recent version of our baseband boards realizes a 2-band operation allowing parallel spectra acquisition for two frequency bands. Accordingly these baseband boards have the possibility to connect two TXs or two RXs. This allows us to increase the bandwidth of the spectroscopy system to about 50 GHz. The PLL devices (Analog Device ADF4159) are now integrated in the baseband board. Thus, 4 fractional-N PLLs are used for the 2-band operation. A single internal reference clock of 100 MHz is placed on the baseband board to allow synchronization of the four PLLs, and it is used as an external reference clock for the experimental set up. The 2-band TX/RX chips are bonded on a special plug-in board, which connects the two TXs and two RXs to the baseband board.

B. Experimental set up for gas spectroscopy

The spectroscopic system includes a gas absorption cell with 1.9 m path length, which is located between the

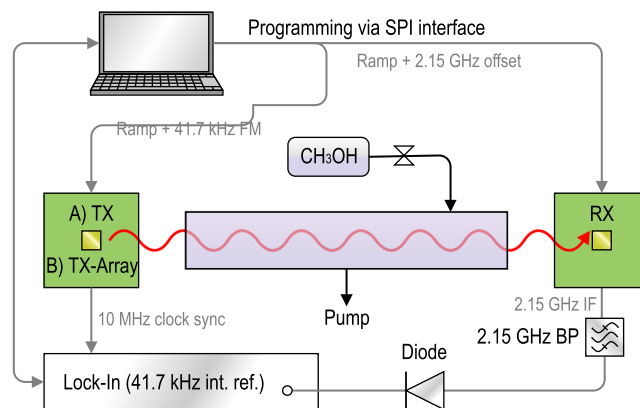


FIG. 9. Block diagram of the spectroscopy system. The frequency ramps for the TX and RX are generated using fractional-N PLLs. The frequency modulation for the TX is performed by the fractional-N PLL generating a superimposed FSK.

TX- and RX-baseband boards.¹¹ Fig. 9 shows the block diagram of the system, and Fig. 10 presents the gas absorption cell with attached TX/RX-baseband boards. The loss of the gas cell was determined to 6 dB.¹¹ Due to the folded path design with glass tube segments of 0.6 m length and 40 mm diameter, the setup including the gas cell and the vacuum pumps is mounted on a compact 450 x 750 mm² base plate. We use a combination of a compact diaphragm pump (Pfeiffer MVP006) and a compact commercially available turbomolecular pump (Pfeiffer HiPace10). The coupling of the radiation from the TX into the absorption cell and from there into the RX is realized by two plano-convex high-density polyethylene (HDPE) lenses with focal lengths of 40 mm which also serve as entrance and exit windows of the gas cell. The TX- and RX-chips are positioned within a 40 mm distance to the lenses.

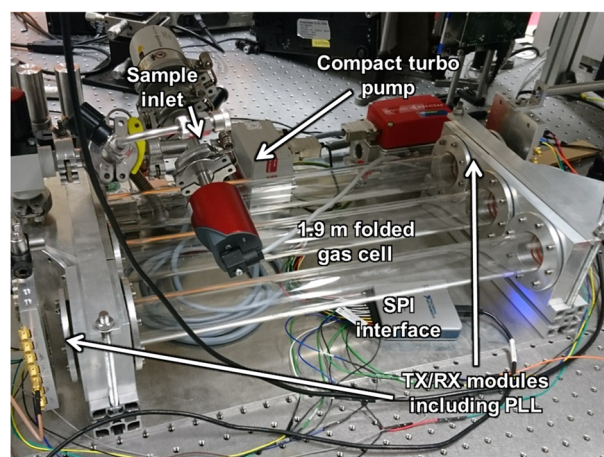


FIG. 10. Spectroscopy setup with folded gas cell, vacuum pump in the background, and TX- and RX-baseband boards mounted close to both ends of the absorption cell.

The second harmonic content ($2f$) of the absorption spectrum was obtained by detecting the IF power of the RX using a diode power sensor (Agilent 8472B) connected to a lock-in amplifier (LIA, Zurich Instruments HF2LI). The IF-signal of the RX at an IF-frequency of 2.15 GHz is connected to an external bandpass at this frequency (mini circuits ZX75BP-2150+). We have used this relatively high IF-frequency to avoid a distortion of the IF-signal due to spurious signals, which are related to the strong $1/64$ frequency divider signal of the local oscillator and its harmonics as well as mixing products of these signals with the IF-signal.

The measurement is controlled by a PC using a LabVIEW program for data acquisition. The frequency ramps for the LOs of the TX and RX are generated using an SPI interface between the LabVIEW program and the corresponding two fractional-N PLL devices (Analog Devices ADF4159), which are applied to tune the VCOs of the TX and RX. The frequency modulation (FM) for the TX is performed by a fractional-N PLL generating a superimposed FSK.

IV. RESULTS OF SPECTROSCOPIC MEASUREMENTS

With the setup described above, CH_3OH spectra were measured for characterization of the TX and RX performance. As a benchmark, we determined the SNR value of a CH_3OH absorption line at 247.6 GHz at a pressure of 5 Pa.

Fig. 11a shows the spectrum measured with the TX-array. On the right, in Fig. 11b, a snippet of the spectrum indicated by the red box is shown. The line at 248 GHz is weaker than our reference line by two orders of magnitude. The very weak line close to it is not listed in the JPL database.²² The full spectrum was taken with an acquisition time of 24 s and the integration time of the lock-in amplifier was 2 ms. The amplitude of the 41.7 kHz frequency modulation was 1 MHz. The modulation was realized by FSK. Previously, we compared FSK and sine wave modulation and there was no considerable difference in the line shape or the SNR normalized to the integration time.²³

According to the JPL molecular spectral database²² this line has an integrated absorption coefficient of $5.7\text{E-}23$ cm which is comparable to the absorption line we measured

in previous publications (with $5.0\text{E-}23$ cm @ 241.7 GHz).¹⁷ All other parameters of the measurements (24 s acquisition time for 1.2 GHz scan range, 41.7 kHz modulation frequency, 1 MHz deviation, 2 ms lock-in integration time) are also comparable with previous measurements. In the first measurement, we used the single TX, which produced an IF signal of -20.3 dBm in the receiver (setup A). For the absorption line at 247.6 GHz, we observed an SNR of 2160 with an RMS noise level of 180 nV. The noise level is dominated by the diode power detector which was determined to 140 nV. When using a 10 dB IF amplification, we observed that the receiver noise becomes more significant and the SNR was only 1600 at a $1\text{ }\mu\text{V}$ noise level. The SNR could not be increased as expected because the diode is already in the nonlinear range with amplification. Thus, in order to increase the SNR, we used the TX-array with a higher output power (setup B) instead of the single TX. With the array, we got an IF power of -10.5 dBm, which is still in the linear range of our RX, see Fig. 8.

The RX behaved linear up to an IF power of -5.2 dBm as determined for the spectroscopy setup with a commercial transmitter from VDI (Virginia Diodes, Inc.) in agreement with the results shown in Fig. 8. With the TX-array, the SNR was determined to 4660 with a noise level of 280 nV. Given the integration time of 2 ms, the baseband noise voltage is 17.7 nV/ $\sqrt{\text{Hz}}$. The corresponding predicted SNR at a 1 Hz bandwidth (0.5 s integration) is $7.4\cdot 10^4$. This is better by a factor of 2.5 compared to Ref. 16, where a baseband SNR of $2.9\cdot 10^4$ was reported for an OCS line which is much stronger. Assuming a linear scaling of the SNR with the pressure (which is in good approximation the case up to 5 Pa – Doppler and pressure broadening linewidths equal at 2 Pa for CH_3OH), with 0.5 s integration an SNR of 1 would be achieved at a pressure of $6.7\cdot 10^{-5}$ Pa. In a 5 Pa sample this corresponds to concentration of 14 ppm that can be detected without any pre-concentration. However, the detection limit is strongly dependent on the molecular species and the line strength of the selected absorption line.

In Ref. 16 sensitivities of 11 ppm and 14 ppm are given for OCS at 279.685 GHz and for Acetonitrile at 294.251 GHz, respectively. The integrated absorption coefficients of these lines ($1.21\cdot 10^{-21}$ cm and $7.07\cdot 10^{-21}$ cm)²² are much stronger than

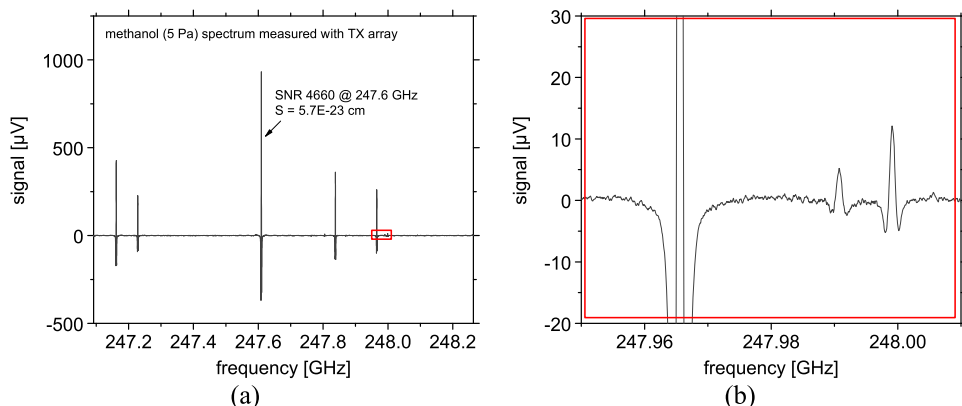


FIG. 11. $2f$ spectrum of CH_3OH measured with TX-array. The reference frequency ramp with superimposed FSK is delivered by fractional-N PLL. The measurement time is 24 s. The SNR is 4660 for the absorption line at 247.6 GHz: a) Full spectrum, b) Snippet of the spectrum.

TABLE I. Performance of integrated transmitters and receivers used for gas spectroscopy.

	Ref. 16	This work
Technology	65nm CMOS	0.13 μ m SiGe
Lock Range (GHz)	220-330 10x 10GHz-band	243-260 (1-band) 222-270 (2-bands)
EIRP (dBm)	10 at 260GHz on-chip antenna with silicon lens	7 (TX), 18 (TX-array) at 245GHz
PN (dBc/Hz) for TX at 1MHz	-102 signal generator average of 10 bands	-85 LO at 240GHz
NF of RX (dB) (SSB)	14.6-19.5 at 220-330GHz	18 at 245GHz
1dB Compression Point of RX (dBm)	N/A	-10

the methanol line at 247.6 GHz (5.7·10⁻²³ cm) resulting in a peak absorption of 94% and 99%, respectively. For the methanol line at 5 Pa, we simulated peak absorption of 17%. Correspondingly, our expected sensitivities for OCS and Acetonitrile are approximately 2 – 3 ppm. The difference in Doppler linewidths is not taken into account.

With our 220 – 330 GHz laboratory spectrometer utilizing a commercial TX/RX system from Virginia Diodes Inc. (WR3.4AMC-I and WR3.4MixAMC-I with diagonal horn antennas) we observed an SNR of 7900 with comparable measurement parameters (same frequency sweep rate, same integration time, same frequency modulation amplitude) for a similar line (5.0E-23 cm @ 241.7 GHz).

V. DISCUSSION

The Table I compares the main parameters of the TX and RX of our gas spectroscopy system in SiGe BiCMOS with a recent system, which uses TX and RX circuits in CMOS technology.¹⁵ A dual-frequency-comb architecture was applied, which enables scalability to higher bandwidth with extended cascading of channels (10 x 10 GHz-band). Two high-performance external signal sources at 45.0 – 46.7 GHz and an external 10 GHz signal were used for this system. This explains the very low phase noise (PN) of the TX compared to our results for the more compact system with internal LO. However, the PN specification of our internal LO, see Table I, is sufficient to detect Doppler-limited absorption lines of gas molecules (e.g. ~ 500 kHz for methanol) by our spectroscopy system.

Previously we have reported absorption spectra of CH₃OH in the range 241 – 242 GHz at a gas pressure of 1.4 Pa with an SNR of 1515 (integration time of 2 ms for each data point) for the absorption line at 241.7 GHz using our TX-array.¹⁷ Here, the SNR increases up to the maximum SNR-value with the square root of the received power, before it saturates and decreases due to a nonlinear operation of the used RX for this range of input power. Now, we have implemented an RX with a 1dB compression point of -10 dBm, which works in the linear region for the TX-array, and does not limit the sensitivity of the system.

For our TX/RX system, the noise level of the signal in the spectrum is dominated by the diode power detector for the IF signal of our RX, and not by noise contributions from the RX and TX, as found and discussed in detail for the CMOS spectroscopy system in Ref. 16. The implementation of our RX/TX chips allowed us to increase the detection sensitivity of our TX/RX system to a level, which is higher by factor 5 – 6 compared to recent spectroscopic results reported for the TX/RX system in CMOS.¹⁶ This is a significant improvement of our TX/RX system compared to the system in Ref. 16.

The parallelism of the 10x 10 GHz spectrum acquisition with the CMOS based system gives advantage compared to a conventional single frequency sweep.¹⁵ However, in case of a dedicated frequency sweep for only selected absorption lines as realized in our system, using a fractional-N PLL for tuning the local oscillator, the acquisition time is considerably reduced for a single frequency sweep.¹¹ Further, our 2-band frequency system for a bandwidth of 50 GHz, with frequency flexibility in each frequency band, gives even more advantage concerning short acquisition time.

The 2-band operation of our TX/RX system with local oscillators for each frequency band allows a parallel spectra acquisition and therefore a high flexibility of data acquisition for the two frequency-bands. This configuration allows also for switching between preselected frequency-regions in the two bands according to the spectral signature, thus reducing the data acquisition time considerably by a factor up to 10 for each band. Therefore, our system gives significant advantage concerning parallel spectra acquisition compared to the 10-band system described in Ref. 16, which uses only one LO to sweep the frequencies in all bands.

VI. CONCLUSION

Our gas spectroscopy system based on transmitters and receivers in SiGe BiCMOS technology for 222 – 270 GHz reveals a high SNR for the detection of gas absorption lines, which is demonstrated for gaseous CH₃OH. The implementation of a mixer-first receiver with high linearity allows the

use of a relatively large transmitter output power for gas spectroscopy, and hence the realization of a high SNR value. In this case, the SNR is close to a reference value obtained with our system, when using commercial GaAs components for the TX and RX. The frequency range of 222 - 270 GHz enables the detection of a large number of VOCs which are, for example, relevant for breath analysis or for detection of TICs. We will further improve our spectroscopy system in order to increase the signal power at the receiver, and hence the SNR value for the detection of weak absorption lines of these VOCs. This will be achieved by reducing the loss of the gas absorption cell, and by implementing a lens-coupled on-chip antenna for the TX and RX. A gas absorption cell with reduced dimension is also required, to realize a mobile gas spectroscopy system. The integration of a compact pre-concentrator in the system will further help to overcome the limits set by the electronic components, and thus enable a detection sensitivity which is for example required in clinical applications for breath analysis.

ACKNOWLEDGMENTS

This work was supported by Deutsche Forschungsgemeinschaft (DFG) through the DFG project ESSENCE under Grant SPP 1857.

REFERENCES

- ¹I. R. Medvedev, C. Neese, G. M. Plummer, and F. C. De Lucia, "Submillimeter spectroscopy for chemical analysis with absolute specificity," *Opt. Lett.* **35**(10), 1533-1535 (2010).
- ²C. F. Neese, I. R. Medvedev, G. M. Plummer, A. J. Frank, C. D. Ball, and F. C. De Lucia, "Compact submillimeter/terahertz gas sensor with efficient gas collection, preconcentration, and ppt sensitivity," *IEEE Sensors Journal* **21**, 2565-2574 (2012).
- ³A. M. Fosnight, B. L. Moran, and I. R. Medvedev, "Chemical analysis of exhaled human breath using a terahertz spectroscopic approach," *Appl. Phys. Lett.* **103**, 133703 (2013).
- ⁴F. C. de Lucia, "Spectroscopy in the terahertz spectral region," in: *Sensing with terahertz radiation*, Springer, Berlin, Heidelberg, New York (2002).
- ⁵E. Bründermann, H.-W. Hübers, and M. F. Kimmitt, *Terahertz Techniques* (Springer, Berlin, Heidelberg, New-York, 2011).
- ⁶H.-W. Hübers, S. G. Pavlov, H. Richter, A. D. Semenov, L. Mahler, A. Tredicucci, H. E. Beere, and D. A. Ritchie, "High-resolution gas phase spectroscopy with a distributed feedback terahertz quantum cascade laser," *Appl. Phys. Lett.* **89**, 061115 (2006).
- ⁷H.-W. Hübers, M. F. Kimmitt, N. Hiromoto, and E. Bründermann, "Terahertz spectroscopy: System and sensitivity considerations," *IEEE Trans. on Science and Technol.* **1**, 321-331 (2011).
- ⁸I. R. Medvedev, R. Schueler, J. Thomas, O. Kenneth, H.-J. Nam, N. Sharma, Q. Zhong, D. Lary, and P. Raskin, "Analysis of exhaled human breath via terahertz molecular spectroscopy," in *IEEE Proc. Infrared, Millimeter and Terahertz Wave (IRMMW-THz)*, Copenhagen, Denmark, Sept. 2016, pp. 1-2.
- ⁹K. Schmalz, R. Wang, W. Debski, H. Gulan, J. Borngräber, P. Neumaier, and H.-W. Hübers, "245 GHz SiGe sensor system for gas spectroscopy," *Int. J. of Microwave and Wireless Technologies* **7**(3/4), 271-278 (2015).
- ¹⁰K. Schmalz, J. Borngräber, W. Debski, M. Elkhoully, R. Wang, P. Neumaier, and H.-W. Hübers, "245 GHz SiGe transmitter array for gas spectroscopy," *IEEE Trans. on Terahertz Science and Technology* **6**(2), 318-327 (2016).
- ¹¹K. Schmalz, N. Rothbart, P. F.-X. Neumaier, J. Borngräber, H.-W. Hübers, and D. Kissinger, "Gas spectroscopy system for breath analysis at mm-wave/THz using SiGe BiCMOS circuits," *IEEE Trans. on Microwave Theory and Techniques* **65**(5), 1807-1818 (2017).
- ¹²K. Schmalz, Y. Mao, J. Borngräber, P. Neumaier, and H.-W. Hübers, "Tunable 245 GHz transmitter and receiver in SiGe technology for gas spectroscopy," *Electronics Letters* **50**(12), 881-882 (2014).
- ¹³K. Schmalz, J. Borngräber, W. Debski, P. Neumaier, R. Wang, and H. W. Hübers, "Tunable 500 GHz transmitter-array in SiGe technology for gas spectroscopy," *Electronics Letters* **51**(3), 257-259 (2015).
- ¹⁴K. Schmalz, J. Borngräber, S. B. Yilmaz, N. Rothbart, D. Kissinger, and H.-W. Hübers, "Gas spectroscopy with 245 GHz circuits in SiGe BiCMOS and frac-N PLL for frequency ramps," in *Proc. IEEE Sensors Conf.*, Orlando, FL, USA, Nov. 2016, pp. 1-4.
- ¹⁵C. Wang and R. Han, "Dual-terahertz-comb spectrometer on CMOS for rapid, wide-range gas detection with absolute specificity," *IEEE Journal of Solid-State Circuits* **52**(12), 3361-3372 (2017).
- ¹⁶C. Wang, B. Perkins, Z. Wang, and R. Han, "Molecular detection for unconcentrated gas with ppm sensitivity using dual-THz-comb spectrometer in CMOS," *IEEE Transactions on Biomedical Circuits and Systems* **12**(3), 709-721 (2018).
- ¹⁷K. Schmalz, N. Rothbart, J. Borngräber, S. B. Yilmaz, D. Kissinger, and H.-W. Hübers, "Gas spectroscopy system with transmitters and receivers in SiGe BiCMOS for 225-273 GHz," *Proc. SPIE* **10439**, 1043902 (2017).
- ¹⁸N. Rothbart, K. Schmalz, D. Kissinger, and H.-W. Hübers, "Two-channel gas spectroscopy setup around 245 GHz in SiGe BiCMOS technology," in *Proc. 6th EOS Topical Meeting on Terahertz Science & Technology (TST 2018)*, Berlin, Germany, May 2018, pp. -3.
- ¹⁹D. Kissinger, N. Rothbart, K. Schmalz, J. Borngräber, and H.-W. Hübers, "Sensitive millimeter-wave/terahertz gas spectroscopy based on SiGe BiCMOS," in *IEEE Proc. Infrared, Millimeter and Terahertz Wave (IRMMW-THz)*, Nagoya, Japan, Sept. 2018, pp. 1-2.
- ²⁰H. Rucker, B. Heinemann, and A. Fox, "Half-terahertz SiGe BiCMOS technology," in *Proc. IEEE Topical Meeting on Silicon Monolithic Integrated Circuits in RF Systems (SiRF)*, Santa Clara, CA, USA, Jan. 2012, pp. 129-132.
- ²¹M. H. Eissa, A. Awany, M. Ko, K. Schmalz, M. Elkhoully, A. Malignaggi, A. C. Ulusoy, and D. Kissinger, "A 220-275 GHz direct-conversion receiver in 130-nm SiGe:C BiCMOS technology," *IEEE Microwave and Wireless Components Letters* **27**(7), 675-677 (2017).
- ²²H. M. Pickett, R. L. Poynter, E. A. Cohen, M. L. Delitsky, J. C. Pearson, and H. S. P. Müller, "Submillimeter, millimeter, and microwave spectral line catalog," *Journal of Quantitative Spectroscopy and Radiative Transfer* **60**(5), 883-890 (1998).
- ²³N. Rothbart, K. Schmalz, J. Borngräber, D. Kissinger, and H.-W. Hübers, "A compact gas spectroscopy sensor system based on a voltage-frequency-tuned 245 GHz SiGe transmitter and receiver," in *41st International Conference on Infrared, Millimeter, and Terahertz Waves (IRMMW-THz)*, Copenhagen, Denmark, 2016.
- ²⁴K. Schmalz, J. Borngräber, B. Heinemann, H. Rucker, and J. C. Scheytt, "A 245 GHz transmitter in SiGe technology," in *IEEE RFIC Symp. Proc.*, Montreal, Canada, 2012, pp. 195-198.